Research Paper

Effects of Tribuloside on Apoptosis and Oxidative Damage of H_2O_2 Treated Human Lens Epithelial Cells *via* Mediating microRNA-335-3p/KLF6 Axis

Y. ZHAO[2]*, XIAN LIU[1,2] AND Q. LIU[1,2]

Department of Ophthalmology, [1]Department of Corneal Transplantation, Affiliated Eye Hospital of Nanchang University, [2]Jiangxi Research Institute of Ophthalmology and Visual Science, Nanchang, Jiangxi Province 330000, China

To explore the protective function and molecular mechanism of tribuloside in hydrogen peroxide-induced apoptosis and oxidative damage of human lens epithelial cells. Cells were divided into control group, hydrogen peroxide group, hydrogen peroxide+tribuloside 1 μg/ml group, hydrogen peroxide+tribuloside 3 μg/ml group, hydrogen peroxide+tribuloside 10 μg/ml group, hydrogen peroxide+microRNA-NC group, hydrogen peroxide+microRNA-335-3p group, hydrogen peroxide+tribuloside+anti-microRNA-335-3p group. Cell counting kit-8 method and flow cytometry were applied for determining cell viability and apoptosis. Malondialdehyde level, catalase and superoxide dismutase activities were determined using kits. Reverse transcription-quantitative polymerase chain reaction was used for microRNA-335-3p quantification. Kriippel-like factor 6 expression was examined *via* Western blot. Target regulation relationship of miR-335-3p and Kriippel-like factor 6 was analyzed *via* dual-luciferase report assay. Contrasted with the control group, cell viability, catalase and superoxide dismutase viabilities, and microRNA-335-3p expression were significantly reduced in hydrogen peroxide group ($p<0.05$), while apoptosis, malondialdehyde and Kriippel-like factor 6 levels were overtly promoted ($p<0.05$). Contrasted to hydrogen peroxide group, cell viability, catalase and superoxide dismutase activities, and microRNA-335-3p expression in hydrogen peroxide+tribuloside 1 μg/ml group, hydrogen peroxide+tribuloside 3 μg/ml group, hydrogen peroxide+tribuloside 10 μg/ml group were obviously enhanced ($p<0.05$), but cell apoptosis, malondialdehyde level and Kriippel-like factor 6 protein level were suppressed ($p<0.05$). Relative to hydrogen peroxide+microRNA-NC group, cell viability, catalase and superoxide dismutase activities in hydrogen peroxide+microRNA-335-3p group were markedly elevated ($p<0.05$), whereas apoptosis inhibition, malondialdehyde level reduction and Kriippel-like factor 6 protein down-regulation were induced ($p<0.05$). Compared with hydrogen peroxide+tribuloside group, cell viability, catalase and superoxide dismutase activities in hydrogen peroxide+tribuloside+anti-microRNA-335-3p group were signally inhibited ($p<0.05$), but apoptosis, malondialdehyde and Kriippel-like factor 6 levels were accelerated ($p<0.05$). MicroRNA-335-3p directly interacted with Kriippel-like factor 6. Tribuloside could attenuate apoptosis and oxidative damage in hydrogen peroxide-induced cataract model, which was related to microRNA-335-3p/Kriippel-like factor 6 axis.

Key words: Tribuloside, hydrogen peroxide, epithelial cells, apoptosis, oxidative injury, microRNA-335-3p, Kriippel-like factor 6

Cataract is a common disease with the highest incidence of impaired vision in the elderly, as the primary cause of blindness in the worldwide. Although patients can see again after cataract extraction and intraocular lens implantation, there are still risks of wound leakage, corneal abrasions and high eye pressure[1]. Reactive Oxygen Species (ROS)-caused oxidative stress is the main factor leading to the occurrence of cataract. Oxidative

Accepted 29 September 2023
Revised 29 November 2022
Received 02 March 2022
Indian J Pharm Sci 2023;85(5):1504-1511

***Address for correspondence**
E-mail: zhaoyao2048@126.com

damage can activate a variety of signaling pathways such as caspases, and induce lens epithelial cell apoptosis to result in lens opacity and cataract occurrence[2,3]. Thus, protecting lens epithelial cells against apoptosis and oxidative damage is an important strategy to delay cataract formation.

Tribuloside is the main active ingredient of *Tribulus terrestris L*. with anti-cancer, anti-aging, hypotensive, and hypolipidemic biological activities[4]. It has been reported that tribuloside might reduce Hydrogen peroxide (H_2O_2)-induced oxidative damage of PC12 cells by stabilizing mitochondrial membrane potential and inhibiting cell apoptosis[5]. Tribuloside was shown to enhance survival rate and cell growth of rat retinal ganglion cells *in vitro*[6]. However, the effects of tribuloside on lens epithelial cells in cataract are still unknown.

MicroRNAs (miRNAs) exhibit the regulatory roles in eye diseases by messenger Ribonucleic Acid (mRNA) degradation[7]. The previous study has demonstrated that miR-335-3p was associated with nuclear opacity grade of lens in nuclear cataract patients, and it could be a key factor involved in oxidative damage of lens epithelial cells[8]. Kriippel-Like Factor 6 (KLF6) was reported to aggravate UV-B-induced apoptosis of lens epithelial cells *via* inducing ROS accumulation[9]. Target relation between miR-335-3p and KLF6 remains to be investigated.

Herein, this study was performed for investigating the functional mechanism of tribuloside in H_2O_2-induced cataract cell model with miR-335-3p/KLF6 axis as the entry point.

MATERIALS AND METHODS

Materials and reagents:

HLE-B3 (Human Lens Epithelial cell line) was provided by American Type Culture Collection (United States of America (USA)). Tribuloside (purity 98 %, batch No. 20191210, a mass concentration of 20 mg/ml mother solution prepared with dimethyl sulfoxide was diluted to the required concentration with culture solution) was purchased from Herbpurify (Chengdu, China). Cell Counting Kit-8 (CCK-8) and miRNA reverse transcription kit were acquired from Vazyme (Nanjing, China). The miRNA fluorescence quantitative detection kit was obtained from Cellregen (Beijing, China). Apoptosis detection kit was bought from Yeasen (Shanghai, China). Malondialdehyde (MDA) content determination kit, Radioimmunoassay (RIPA) buffer, Superoxide Dismutase (SOD) activity kit, Catalase (CAT) activity kit, Bicinchoninic Acid (BCA) protein concentration determination kit were bought from Solarbio (Beijing, China). Luciferase psi-CHECK-2 vector, miR-335-3p mimic (miR-335-3p), miR-NC, and miR-335-3p inhibitor (anti-miR-335-3p) were acquired from Ribobio (Guangzhou, China). Murine Glyceraldehyde 3-Phosphate Dehydrogenase (GAPDH) monoclonal antibody (sc-47724), murine KLF6 monoclonal antibody (sc-134374) and goat anti-mouse IgG secondary antibody (sc-2005) were bought from Santa Cruz (USA).

Cell culture and H_2O_2 induction:

Cells were cultivated with high-glucose Dulbecco's Modified Eagle Medium (DMEM) medium in a constant temperature (37°) incubator containing 5 % Carbon dioxide (CO_2), followed by changing cell medium every day. When cell confluence reached 80 %, cell passage by 1:2 ratio was performed after digestion with trypsin. 5×10^3 cells at the third generation were inoculated into each well of 96-well plates. After incubation with H_2O_2 (0, 50, 100, 200, 400 μmol/l) for 24 h[10], cells were added with 10 μl/well CCK-8 for 2 h and Optical Density (OD) at 450 nm was measured in each well under a microplate reader. According to cell viability, 100 μmol/l H_2O_2 was selected as the working concentration.

Experimental groups:

Randomly, cells were classified into the different groups. Control group HLE-B3 cells in normal culture. H_2O_2 group cells with 100 μmol/l H_2O_2 treatment for 24 h. H_2O_2+tribuloside 1 μg/ml group, H_2O_2+tribuloside 3 μg/ml group, or H_2O_2+tribuloside 10 μg/ml group cells with treatment of 100 μmol/l H_2O_2 and 1 μg/ml, 3 μg/ml or 10 μg/ml tribuloside for 24 h[5]. H_2O_2+miR-NC group and H_2O_2+miR-335-3p group cells with miR-NC or miR-335-3p transfection were exposed to 100 μmol/L H_2O_2 for 24 h. H_2O_2+tribuloside+anti-miR-335-3p group, anti-miR-335-3p-transfected cells were performed with 24 h of 100 μmol/L H_2O_2 incubation. Cell transfection was implemented

following Lipofectamine 3000, then cells were harvested after 48 h for the further assays.

CCK-8 method for cell viability:

96-well plates were seeded with 5×10^3 cells/well of transfected HLE-B3 cells, miR-NC transfected cells, miR-335-3p or anti-miR-335-3p transfected cells. Subsequently, cells were hatched with H_2O_2 and/or tribuloside for 24 h. After incubation of CCK-8 working solution (10 µl of each well) for 2 h, OD detection was administrated under the microplate reader.

Flow cytometry for cell apoptosis:

Cell concentration was adjusted to 2×10^4 cells/ml by resuspending HLE-B3 cells in 500 µl 1× binding buffer. Cell suspension was pipetted with 5 µl Annexin V-Fluorescein Isothiocyante (FITC) and 5 µl Propidium Iodide (PI) (25°, 15 min) away from light. Apoptotic cells of each group were examined through flow cytometry.

Kits for MDA, CAT and SOD detection:

1×10^6 cells HLE-B3 was added with 1 mL extract solution, and the cells were ruptured by 200 W ultrasound (for 3 s, an interval of 10 s, repetition for 30 times). After centrifugation at ultra-low temperature (10 000 rpm, 10 min), cell supernatant was collected for detecting MDA content, CAT and SOD activities according to manuals of corresponding kits.

RT-qPCR for miR-335-3p expression:

TRIzol reagent was employed for extracting total RNA of each group, followed by reverse transcription into complimentary Deoxyribonucleic Acid (cDNA) *via* miRNA reverse transcription kit and expression analysis through miRNA fluorescence quantitative detection kit. $2^{-\Delta\Delta Ct}$ method was utilized for miR-335-3p relative expression calculation. The primer sequences were as follows; miR-335-3p, sense 5′-UUUUUCAUUAUUGCUCCUGACC-3' and antisense 5′-CCAGTCTCAGGGTCCGAGGTATTC-3′; U6, sense 5′-CTCGCTTCGGCAGCACA-3′ and antisense 5′-AACGCTTCACGAATTTGCGT-3′.

Western blot for KLF6 protein analysis:

The protein samples were extracted employing RIPA buffer and quantified by BCA kit. 40 µg denatured proteins were isolated by Sodium Dodecyl-Sulfate Polyacrylamide Gel Electrophoresis (SDS-PAGE) (100 V, 90 min) and transferred to PVDF membrane by a wet transmembrane device (20 mA). After sealing with 5 % skim milk, anti-KLF6 (1:200) and endogenous reference anti-GAPDH (1:500) were incubated to membranes at 4° overnight. After 1 h of incubation with the secondary antibody (1:2000), then blots were presented by Chemiluminescence kit. Relative protein expression of KLF6 was represented as KLF6/GAPDH band gray value measured by ImageJ software.

Dual-luciferase reporter assay for miR-335-5p and KLF6 target relation analysis:

TargetScan was utilized for target binding prediction of miR-335-3p and KLF6. Wild-Type (WT) sequence of KLF6 containing miR-335-3p binding region was constructed into psi-CHECK-2 plasmid to generate luciferase reporter vector WT-KLF6. Also, Mutated (MUT) KLF6 sequence containing miR-335-3p binding site was used for MUT-KLF6 construction. Luciferase constructs and miR-335-3p or miR-NC were co-transfected for 48 h, relative luciferase activity examination by dual-luciferase activity system was performed with Renilla luciferase as the internal control.

Statistical analysis:

Experiments were independently administrated for 3 times with 3 repetitions of each group. Data were represented as mean±standard deviation (x±s). For two groups, difference was assessed using independent sample t test. For multiple groups, one-way Analysis of Variance (ANOVA) followed by Tukey test was used for difference analysis. $p<0.05$ was defined as a significant difference.

RESULTS AND DISCUSSION

HLE-B3 cells were disposed with different concentrations of H_2O_2. Compared with 0 µmol/l group, cell viability was signally reduced in 50, 100, 200 and 400 µmol/l groups ($p<0.05$), as exhibited in Table 1.

Relative to control group, cell viability, CAT and SOD activities in H_2O_2 group were markedly lessened ($p<0.05$) but apoptosis rate and MDA level were elevated ($p<0.05$). HLE-B3 cell activity, CAT

activity and SOD activity of H_2O_2+tribuloside 1 μg/ml group, H_2O_2+tribuloside 3 μg/ml group or H_2O_2+tribuloside 10 μg/ml group were gradually elevated ($p<0.05$), while apoptotic cells and MDA level were decreased ($p<0.05$) by comparison with H_2O_2 group, as depicted in fig. 1 and Table 2.

TABLE 1: CELL VIABILITY DETECTION IN DIFFERENT CONCENTRATIONS OF H_2O_2-TREATED HLE-B3 (x±s, n=9)

H_2O_2 concentration (μmol/l)	OD value
0	1.27±0.06
50	0.78±0.05[a]
100	0.63±0.04[ab]
200	0.37±0.03[abc]
400	0.24±0.01[abcd]
F	837.776
p	0.000

Note: Contrasted to 0 μmol/l group, [a]$p<0.05$; contrasted to 50 μmol/l group, [b]$p<0.05$; contrasted to 100 μmol/l group, [c]$p<0.05$ and contrasted to 200 μmol/l group, [d]$p<0.05$

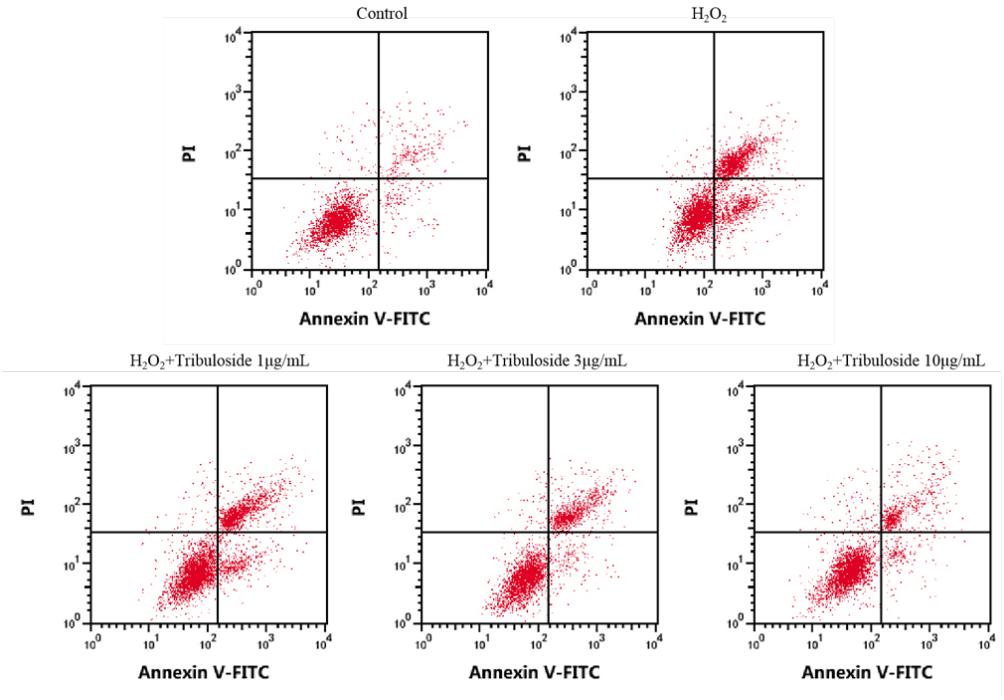

Fig. 1: Tribuloside inhibited apoptosis of H_2O_2-induced HLE-B3 cells

TABLE 2: DETECTION OF VIABILITY, APOPTOSIS AND OXIDATIVE INJURY AFTER H_2O_2 AND TRIBULOSIDE TREATMENT (x±s, n=9)

Group	OD value	Apoptosis rate (%)	CAT (U/ml)	MDA (nmol/ml)	SOD (U/ml)
Control	1.26±0.06	6.56±0.23	116.12±6.39	55.03±1.92	170.63±7.56
H_2O_2	0.58±0.03[a]	23.30±0.78[a]	32.84±1.16[a]	270.63±9.89[a]	23.46±1.27[a]
H_2O_2+tribuloside 1 μg/ml	0.73±0.04[b]	20.29±0.63[b]	44.18±2.12[b]	222.51±10.02[b]	45.59±1.77[b]
H_2O_2+tribuloside 3 μg/ml	0.95±0.05[bc]	16.45±0.56[bc]	68.02±3.13[bc]	153.07±7.74[bc]	93.86±4.00b[c]
H_2O_2+tribuloside 10 μg/ml	1.16±0.06[bcd]	11.67±0.45[bcd]	94.36±4.19[bcd]	83.73±4.35[bcd]	150.62±7.82[bcd]
F	299.25	1280.29	724.289	1321.86	1323.39
p	0.000	0.000	0.000	0.000	0.000

Note: Relative to control group, [a]$p<0.05$; relative to H_2O_2 group, [b]$p<0.05$; relative to H_2O_2+tribuloside 1 μg/ml group, [c]$p<0.05$ and relative to H_2O_2+tribuloside 3 μg/ml group, [d]$p<0.05$

Relative to control group, miR-335-3p was down-regulated ($p<0.05$) and KLF6 protein up-regulation was significant ($p<0.05$) in H_2O_2 group. Relative to H_2O_2 group, miR-335-3p expression was elevated ($p<0.05$) and KLF6 protein reduction was induced ($p<0.05$) in H_2O_2+tribuloside 1 µg/ml group, H_2O_2+tribuloside 3 µg/ml group and H_2O_2+tribuloside 10 µg/ml group, as exhibited in fig. 2 and Table 3.

Target scan analysis showed that KLF6 3'-UTR contained miR-335-3p binding region, as indicated in fig. 3. Significantly, miR-335-3p and WT-KLF6 co-transfection resulted in relative luciferase activity inhibition compared with miR-NC and WT-KLF6 co-transfection ($p<0.05$). There was no statistical significance in luciferase detection of MUT-KLF6 group with transfection of miR-NC and miR-335-3p, as shown in Table 4.

Contrasted to H_2O_2 group and H_2O_2+miR-NC group, miR-335-3p level was notably increased in H_2O_2+miR-335-3p group ($p<0.05$). Cell viability, CAT and SOD activities were enhanced ($p<0.05$), while cell apoptosis, MDA and KLF6 levels were overtly inhibited ($p<0.05$), as displayed in fig. 4 and Table 5.

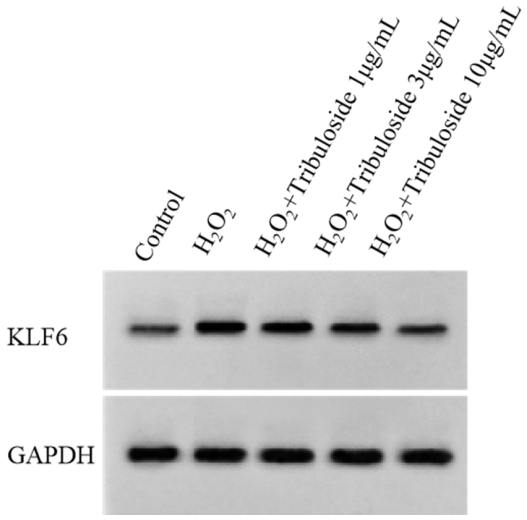

Fig. 2: Effect of tribuloside on KLF6 protein level after H_2O_2 treatment

TABLE 3: DETECTION OF miR-335-3p AND KLF6 AFTER H_2O_2 AND TRIBULOSIDE TREATMENT (x±s, n=9)

Group	miR-335-3p	KLF6
Control	1.00±0.00	0.14±0.01
H_2O_2	0.17±0.01[a]	0.79±0.06[a]
H_2O_2+tribuloside 1 µg/ml	0.35±0.02[b]	0.59±0.04[b]
H_2O_2+tribuloside 3 µg/ml	0.59±0.04[bc]	0.38±0.03[bc]
H_2O_2+tribuloside 10 µg/ml	0.82±0.05[bcd]	0.19±0.01[bcd]
F	1112.57	533.357
p	0.000	0.000

Note: Contrasted with control group, [a]$p<0.05$; contrasted with H_2O_2 group, [b]$p<0.05$; contrasted with H_2O_2+tribuloside 1 µg/ml group, [c]$p<0.05$ and contrasted with H_2O_2+tribuloside 3 µg/ml group, [d]$p<0.05$

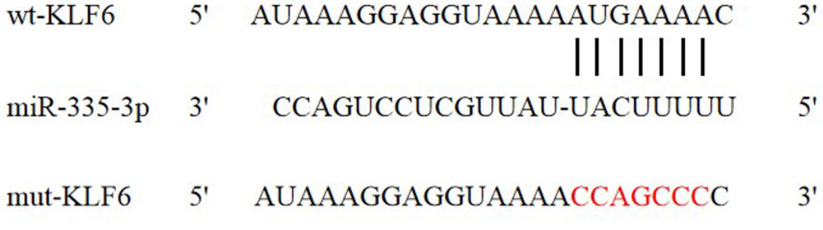

Fig. 3: Complementary sequences between miR-335-3p and KLF6

TABLE 4: EXAMINATION OF RELATIVE LUCIFERASE ACTIVITY (x±s, n=9)

Group	WT-KLF6	MUT-KLF6
miR-NC	1.01±0.09	1.02±0.09
miR-335-3p	0.14±0.01[a]	0.98±0.07
t	28.823	1.052
p	0.000	0.308

Note: Contrasted with miR-NC group, [a]p<0.05

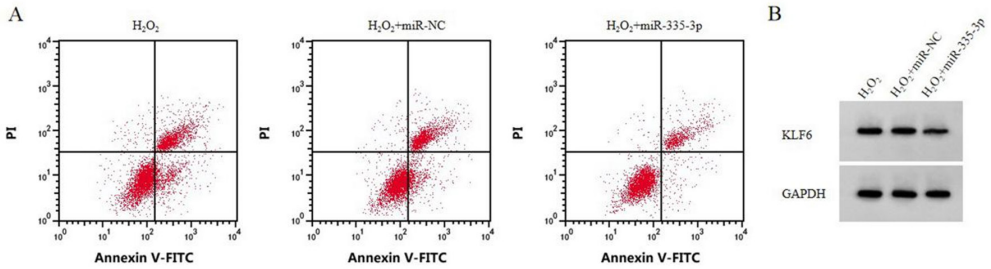

Fig. 4: Effects of miR-335-3p overexpression on apoptosis and KLF6 protein level, (A): Overexpression of miR-335-3p suppressed H_2O_2-induced HLE-B3 cell apoptosis and (B): Overexpression of miR-335-3p reduced KLF6 protein level after H_2O_2 treatment

TABLE 5: DETECTION OF APOPTOSIS AND OXIDATIVE INDICATORS IN H_2O_2-TREATED CELLS AFTER miR-335-3p UP-REGULATION (x±s, n=9)

Group	miR-335-3p	KLF6	OD value	Apoptosis rate (%)	CAT (U/ml)	MDA (nmol/ml)	SOD (U/ml)
H_2O_2	1.00±0.00	0.78±0.06	0.58±0.04	23.33±0.68	32.79±0.99	271.20±15.55	23.49±1.31
H_2O_2+miR-NC	1.01±0.01	0.79±0.06	0.61±0.05	23.51±0.64	32.86±1.06	273.86±14.73	23.55±1.07
H_2O_2+miR-335-3p	4.48±0.09[ab]	0.25±0.02[ab]	1.04±0.06[ab]	13.31±0.42[ab]	78.26±4.20[ab]	106.56±10.39[ab]	123.50±6.32[ab]
F	13253.8	339.04	232.247	877.649	941.013	437.533	2101.8
P	0.000	0.000	0.000	0.000	0.000	0.000	0.000

Note: Contrasted with H_2O_2 group, [a]p<0.05 and contrasted with H_2O_2+miR-NC group, [b]p<0.05

Compared with H_2O_2 group, miR-335-3p level, cell viability, CAT and SOD activity in H_2O_2+tribuloside group were markedly elevated (p<0.05) while apoptotic cells, MDA level and KLF6 protein level were repressed (p<0.05). Contrasted to H_2O_2+tribuloside group, miR-335-3p down-regulation was detected in H_2O_2+tribuloside+anti-miR-335-3p group (p<0.05). Cell viability, CAT and SOD activities were reduced (p<0.05), whereas cell apoptosis, MDA and KLF6 levels were enhanced (p<0.05), as indicated in fig. 5 and Table 6.

Oxidative stress induced by ROS, such as H_2O_2 is considered as a pivotal mediator to result in lens epithelial cell apoptosis in cataract[11]. In this study, H_2O_2 was employed to mimic oxidative damage in cataract cell model. HLE-B3 cell viability was significantly reduced after exposure to H_2O_2, and 100 µmol/l H_2O_2 was selected as the working concentration when cell viability was close to 50 %. CAT and SOD are important antioxidant enzymes for clearing ROS. Balance breakdown between ROS production and clearance can trigger aberrant apoptosis and oxidative injury of lens epithelial cells, which is associated with the occurrence of cataract[12]. Li *et al.*[13] reported that tribuloside improved nerve cell injury after experimental cerebral hemorrhage in rats, maybe by the anti-free radical mechanism. Our results demonstrated that induction of H_2O_2 can enhance cell apoptosis and the level of MDA (the end product of lipid peroxidation), then tribuloside reversed cell damage in a concentration-dependent manner. Tribuloside could enhance cell viability, antioxidative capacity and inhibit apoptosis of HLEB-3 cells, thus protecting from H_2O_2-induced cell damage.

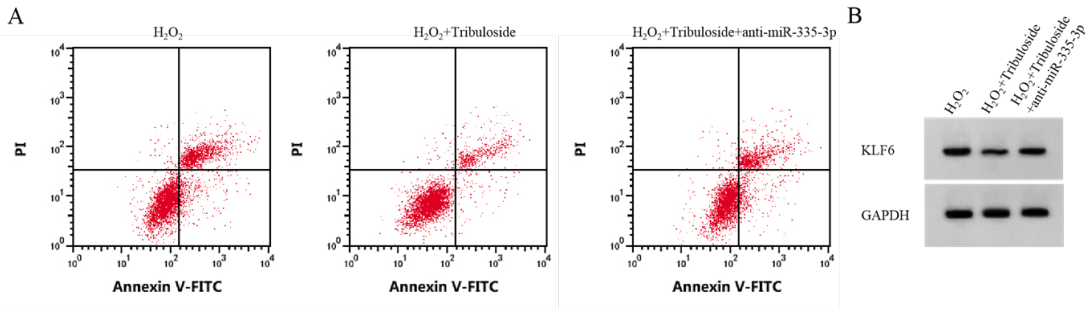

Fig. 5: Inhibition of miR-335-3p counteracted the regulation of tribuloside in cell apoptosis and KLF6 protein level, (A): Reduction of miR-335-3p recovered the inhibitory influence of tribuloside on HLE-B3 cell apoptosis and (B): Inhibition of miR-335-3p attenuated KLF6 protein regulation by tribuloside in HLE-B3 cells

TABLE 6: DOWN-REGULATION OF miR-335-3p RESTORED THE INFLUENCES OF TRIBULOSIDE ON CELL ACTIVITY, APOPTOSIS AND OXIDATIVE STRESS OF H_2O_2-INDUCED HLE-B3 CELLS (x±s, n=9)

Group	miR-335-3p	KLF6	OD value	Apoptosis rate (%)	CAT (U/ml)	MDA (nmol/ml)	SOD (U/ml)
H_2O_2	1.00±0.00	0.77±0.07	0.60±0.04	23.36±0.96	32.89±0.97	273.87±15.29	23.52±1.14
H_2O_2+tribuloside	4.85±0.29[a]	0.19±0.02[a]	1.18±0.05[a]	11.72±0.51[a]	95.24±5.21[a]	83.56±4.76[a]	150.89±9.57[a]
H_2O_2+tribuloside+anti-miR-335-3p	1.53±0.11[b]	0.61±0.04[b]	0.70±0.05[b]	20.40±0.86[b]	42.03±3.27[b]	233.18±10.53[b]	35.47±3.21[b]
F	1222.101	351.130	393.273	514.324	789.384	1549.234	1294.665
p	0.000	0.000	0.000	0.000	0.000	0.000	0.000

Note: Relative to H_2O_2 group, [a]p<0.05 and relative to H_2O_2+tribuloside+anti-miR-335-3p group, [b]p<0.05

The short miRNAs can induce target gene down-regulation by acting on the 3'-UTR of mRNAs, consequently participating in the various kinds of biological processes[14]. Research evidence showed that miRNA expression was changed after oxidative stress was induced in lens epithelial cells[15]. H_2O_2 treatment down-regulated miR-182-5p in HLE-B3 cells, and miR-182-5p level increase protected against cell damage induced by H_2O_2 through directly targeting NOX4[16]. Wang *et al.* stated that miR-34a-5p restrained oxidative stress by reducing GPX3 in lens epithelial cells[17]. miR-23a-3p regulated lens epithelial cell proliferation and apoptosis through degrading Bcl-2 level[18]. Reduction of miR-335-3p level was associated with ischemic neuronal injury, and circTLK1 knockdown ameliorated neuronal injury induced by glucose and oxygen deprivation/reoxygenation *via* up-regulating miR-335-3p[19]. Through inhibiting the expression of ATG3 (an autophagy-related gene), miR-335-3p could suppresses retinal ganglionic cell apoptosis to prevent the progression of glaucoma[20]. Consistent with the results of previous studies, this study affirmed the significantly down-regulation of miR-335-3p after H_2O_2 treatment in HLE-B3 cells. In addition, miR-335-3p overexpression enhanced cell viability and abated H_2O_2-induced apoptosis and oxidative injury. Therefore, miR-335-3p worked as protective factor in cell model of cataract.

KLF6 is an anti-tumor gene implicated in cell proliferation and apoptosis[21]. A pervious study manifested that KLF6 overexpression inhibited proliferation ability of rat lens epithelial cells[22]. KLF6 was affirmed to promote UV-induced apoptosis by triggering endoplasmic reticulum stress in lens epithelial cells[23]. Moreover, miR-181 enhanced retinal endothelial cell migration in diabetic retinopathy through binding to KLF6[24]. miR-124-3p significantly weakened H_2O_2-aroused apoptosis acceleration and viability inhibition *via* the targeted regulation of KLF6 in HLE-B3 cells[25]. Yin *et al.*[26] found that miR-22-3p mediated cell apoptosis through down-regulating KLF6 in diabetic cataract. Herein, it was found that KLF6 protein expression was up-regulated after H_2O_2 treatment. More importantly, miR-335-3p directly interacted with KLF6, and the promoting regulation of H_2O_2 in KLF6 was neutralized. Anti-apoptotic and anti-oxidative influences of tribuloside and miR-335-3p were consistent, suggesting that miR-335-3p and downstream target might mediate the protective effect of tribuloside. Further studies manifested that miR-335-3p level suppression impaired the protective influence of tribuloside on H_2O_2-induced HLE-B3 cell damage

and up-regulated KLF6 protein level. Therefore, the regulatory role of tribuloside in H_2O_2-induced cell damage was achieved partly by miR-335-3p/KLF6 axis.

In summary, this study confirmed that tribuloside could attenuate apoptosis and oxidative damage in H_2O_2-induced cataract cell model through regulating miR-335-3p/KLF6 axis. These evidences provide important evidence for the development of tribuloside in treatment of cataract, and discover the potential effective target for the treatment of cataract.

Conflict of interests:

The authors declared no conflict of interests.

REFERENCES

1. Watkinson S, Seewoodhary M. Cataract management: Effect on patients' quality of life. Nurs Standard 2015;29(21):42-8.
2. Braakhuis AJ, Donaldson CI, Lim JC, Donaldson PJ. Nutritional strategies to prevent lens cataract: Current status and future strategies. Nutrients 2019;11(5):1186.
3. Shentu XC, Ping XY, Cheng YL, Zhang X, Tang YL, Tang XJ. Hydrogen peroxide-induced apoptosis of human lens epithelial cells is inhibited by parthenolide. Int J Ophthalmol 2018;11(1):12.
4. Xiao Y, Guan X, Liao G. Research progress on the application of *Tribulus terrestris* saponins to dermatosis. Chin J Hum Sexuality 2023;32(7):108-12.
5. Jiang E, Su X, Li H, Yang S. Protective effect and mechanism research of *Tribulus terrestris* saponins on H_2O_2-induced apoptosis of PC12 cells. Chin Tradit Herbal Drugs 2008;39(9):1368-71.
6. Huang L, Wang L, Ying F, Zeng P. The protective effect of gross saponin of *Tribulus terrestris* on rat retinal ganglion cells *in vitro*. Chin J Chin Ophthalmol 2008;18(2):89-91.
7. Benavides-Aguilar JA, Morales-Rodríguez JI, Ambriz-González H, Ruiz-Manriquez LM, Banerjee A, Pathak S, *et al.* The regulatory role of microRNAs in common eye diseases: A brief review. Front Genet 2023;14:1152110.
8. Wang S, Guo C, Yu M, Ning X, Yan B, Zhao J, *et al.* Identification of H_2O_2 induced oxidative stress associated microRNAs in HLE-B3 cells and their clinical relevance to the progression of age-related nuclear cataract. BMC Ophthalmol 2018;18(1):93.
9. Tian F, Zhao J, Huang L, Xu M, Zhang Z, Teng H, *et al.* Effects of Krüppel-like factor 6 overexpression towards apoptosis of human lens epithelial cells with ultra violetradiation B treatment. Chin J Exp Ophthalmol 2019;37(4):257-62.
10. Ren H, Tao H, Gao Q, Shen W, Niu Z, Zhang J, *et al.* miR-326 antagomir delays the progression of age-related cataract by upregulating FGF1-mediated expression of betaB2-crystallin. Biochem Biophys Res Commun 2018;505(2):505-10.
11. Yang H, Zhao J, Wang Y, Yu X, Pei C. Salvianolic acid A protects cell proliferation, apoptosis, ultrastructural damage and inflammatory reaction of human lens epithelial cells SRA01/04 induced by H_2O_2. Recent Adv Ophthalmol 2018;38(8):724-31.
12. Peng J, Zheng TT, Liang Y, Duan LF, Zhang YD, Wang LJ, *et al.* p-Coumaric acid protects human lens epithelial cells against oxidative stress-induced apoptosis by MAPK signaling. Oxid Med Cell Longev 2018;2018:8549052.
13. Li L, Li J, Li H, Yang S. Protective effects of gross saponins of *Tribulus terrestris* on experimental intracerebral hemorrhage in rats. J Harbin Med Univ 2006;40(2):99-102.
14. Sun M, Li K, Li X, Wang H, Li L, Zheng G. lncRNA TUG1 regulates Smac/DIABLO expression by competitively inhibiting miR-29b and modulates the apoptosis of lens epithelial cells in age-related cataracts. Chin Med J 2023;2022:112.
15. Shi Z, Su Y, Wang F, Liu P. Downregulation of microRNA-181a attenuates hydrogen peroxide-induced human lens epithelial cell apoptosis *in vitro*. Mol Med Rep 2018;17(4):6009-15.
16. Li ZN, Ge MX, Yuan ZF. microRNA-182-5p protects human lens epithelial cells against oxidative stress-induced apoptosis by inhibiting NOX4 and p38 MAPK signalling. BMC Ophthalmol 2020;20(1):1-9.
17. Wang S, Yu M, Yan H, Liu J, Guo C. miR-34a-5p negatively regulates oxidative stress on lens epithelial cells by silencing GPX3–A novel target. Curr Eye Res 2022;47(5):727-34.
18. Yao P, Jiang J, Ma X, Chen Z, Hong Y, Wu Y. miR-23a-3p regulates the proliferation and apoptosis of human lens epithelial cells by targeting Bcl-2 in an *in vitro* model of cataracts. Exp Ther Med 2021;21(5):436.
19. Wu F, Han B, Wu S, Yang L, Leng S, Li M, *et al.* Circular RNA TLK1 aggravates neuronal injury and neurological deficits after ischemic stroke *via* miR-335-3p/TIPARP. J Neurosci 2019;39(37):7369-93.
20. Zhang Q, He C, Li R, Ke Y, Sun K, Wang J. miR-708 and miR-335-3p inhibit the apoptosis of retinal ganglion cells through suppressing autophagy. J Mol Neurosci 2021;71(2):284-92.
21. Cai M, Shao W, Yu H, Hong Y, Shi L. Paeonol inhibits cell proliferation, migration and invasion and induces apoptosis in hepatocellular carcinoma by regulating miR-21-5p/KLF6 axis. Cancer Manag Res 2020;12:5931-43.
22. Su Y, Wang F, Zhou D, Gao W, Hu Q, Cui H, *et al.* Inhibition of proliferation of rat lens epithelial cell by overexpression of KLF6. Mol Vision 2011;17:1080.
23. Tian F, Zhao J, Bu S, Teng H, Yang J, Zhang X, *et al.* KLF6 induces apoptosis in human lens epithelial cells through the ATF4-ATF3-CHOP axis. Drug Des Devel Ther 2020;14:1041-55.
24. Cao J, Zhao C, Gong L, Cheng X, Yang J, Zhu M, *et al.* miR-181 enhances proliferative and migratory potentials of retinal endothelial cells in diabetic retinopathy by targeting KLF6. Curr Eye Res 2022;47(6):882-8.
25. Zhang H, Chen Y, Chen S. Effect of miR-124-3p targeted regulation of KLF6 genes on proliferation and apoptosis of H_2O_2-induced human lens epithelial cells. Recent Adv Ophthalmol 2020;40(2):125-30.
26. Yin X, Chen L, Shen J, Bi Z, Chen C, Zhao X, *et al.* microRNA-22-3p regulates the apoptosis of lens epithelial cells through targeting KLF6 in diabetic cataracts. Transl Vis Sci Technol 2023;12(5):9.